SUPPLEMENTAL INFORMATION

Class IIa Histone Deacetylases are Hormone-activated regulators of FOXO and Mammalian Glucose Homeostasis

SUPPLEMENTAL FIGURES

Figure S1. Validation of Specificity of HDAC Antibodies Used and Assessment of Class IIa HDAC localization and 14-3-3 Binding, Related to Figure 1

(A) Hepa1-6 hepatoma, C2C12 myoblasts, or mouse embryonic fibroblasts (MEF) were infected with adenoviruses bearing hairpin shRNAs against murine HDAC4, HDAC5, or HDAC7 as indicated and immunoblotted with indicated antibodies to detect endogenous HDAC proteins.

(B) FLAG-tagged wild-type, Ser259Ala, Ser498Ala, or Ser259Ala/ Ser498Ala (AA) mutant HDAC5 constructs were transfected in HEK293T cells, immunoprecipitated with anti-FLAG antibody and immunoblotted with the indicated antibodies.

(C) Activation of endogenous AMPK or overexpression of AMPK relocalizes wild-type (WT) HDAC5-GFP, but not Ser259A/Ser498A (AA)-HDAC5-GFP out of the nucleus. U2OS cells were transfected with wild-type GFP-HDAC5 and then treated with 2mM AICAR or 1mM phenformin or vehicle.

(D) U2OS cells were transfected with WT-HDAC5-GFP with or without myc-tagged constitutively active AMPKa2 (1-312) as indicated.

(E) HEK293T cells transfected with indicated myc tagged-AMPKa2 alleles, FLAG-tagged HDAC5 alleles, and GST-14-3-3 and immunoprecipitated with GST-14-3-3 and immunoblotted with indicated antibodies.

(F) Lysates from primary hepatocytes treated with either AMPK agonist A769662 or Vehicle (DMSO) for 1 hr and immunobloted with indicated antibodies.

Figure S2. Forskolin Mimics Glucagon Dependent Effects of De-phosphorylation of the Class IIa HDACs, Related to Figure 2

(A) Mice were starved for 6h and then treated with saline, glucagon (Gluca) for 45 minutes, or refed for 3h. Liver lysates were immunoblotted with indicated antibodies.

(B) Primary mouse hepatocytes were treated with vehicle (DMSO) or 10uM forksolin for indicated times and lysates were immunoblotted with indicated antibodies.

(C) Primary mouse hepatocytes infected with adenovirus expressing GFP-HDAC5 WT were treated with 10uM forskolin or vehicle (DMSO) for indicated times and imaged

(D) Forskolin-induced WT HDAC5-GFP nuclear localization is similar to Ser259Ala/ Ser498Ala HDAC5-GFP constitutive nuclear localization. Primary hepatocytes were infected with adenovirus expressing GFP, WT HDAC5-GFP, or AA-HDAC5-GFP and treated with 10uM forskolin or vehicle (DMSO) for indicated times and imaged.

Figure S3. Glucagon Dependent Transcriptional Effects Require Class IIa HDACs, which Associate with Gluconeogenic Promoters, Related to Figure 3

(A) Top 25 genes whose induction by glucagon is attenuated by HDAC4/5 shRNA compared to scrambled control shRNA. Primary hepatocytes were treated with 10uM Forskolin for 4h. Ratio reflects comparison of 4h Forskolin scrambled control shRNA samples over corresponding 4h forskolin HDAC4/5 shRNA treated samples.

(B) Lysates from primary hepatocytes in parallel cultures to those used in Figure 3B were immunoblotted with indicated antibodies against endogenous proteins.

(C) HDAC4 antibody but not control IgG immunoprecipitates with the promoter proximal region of the murine G6Pase promoter. Primary hepatocytes were treated with glucagon as indicated then subject to chromatin immunoprecipitation with the indicated antibodies. Data are shown as mean +/- s.e.m.

(D) HDAC4 ChIP at -209 region of G6Pase locus in cells infected with scrambled (scram) or HDAC4/5/7 shRNA in cells treated with 100nM glucagon for 1h where indicated. Data are shown as mean +/- s.e.m. (n= 4) * $p < 0.05$, Student's t-test, comparison between Glucagon treated scramble shRNA and Glucagon treated HDAC4/5/7 shRNA samples.

Figure S4. Class IIa HDACs associate with Foxos and regulate their acetylation on multiple lysines, Related to Figure 4

(A) Primary hepatocytes were transduced with Foxo 3 and Flag- HDAC5 WT or AA adenoviruses and treated with Forskolin (FSK) or Vehicle (VEH) for 1 hr. Lysates were immunoprecipitated for Flag HDAC5 WT or AA and immunoblotted with indicated antibodies.

(B) Assessing acetylation of Foxo 3 with two different Foxo acetylation specific antibodies in primary hepatocytes that are knocked down with either Class IIa HDACs shRNAs or scrambled shRNA.

Figure S5. Class IIa HDACs associate with Class I HDAC3, which mediates Foxo deacetylation, Related to Figure 5

(A) Primary hepatocytes tranduced with GFP-HDAC5 WT and Glucagon treated were immunoprecipitated with anti-GFP and immunoblotted for endogenous Foxo1 and HDAC3.

(B) In vitro deacetylation assays were performed on recombinant GST-FOXO1, which had been prior acetylated in vitro with a recombinant fragment of p300. GST-FOXO1 acetylation is detected using the Foxo1 K259/262/271 acetylation specific antibody. HDAC3 complexed with Ncor deacetylated GST-FOXO1 as seen in Figure 4F and not recombinant HDAC4 or HDAC5. Recombinant SIRT1 serves as positive control. Reactions were ran on SDS-PAGE gel and immunobloted with indicated antibodies.

(C) HEK293T cells were transfected with Myc-Foxo1 WT construct and cells were treated with 1uM TSA and/or 10mM NAM for 2 h. Cell lysates were immunobloted with indicated antibodies.

Figure S6. Loss and Gain of Function of the Class IIa HDACs in Liver Augments Hepatic Glycogen Content and Blood Glucose, Related to Figure 5

(A) Mouse livers knockdowns for Class IIa HDACs or control Scramble shRNA were homogenized and assessed for glycogen content. Data represents the fold change of glycogen content of HDACs shRNA depleated livers compared to control scramble shRNA livers. * Data are shown as mean +/- s.e.m. (n=3). $p<0.05$, Student's t-test.

(B) Nonphosphorylatable HDAC5 modestly increases blood glucose and HDAC4/5/7 shRNA reduces blood glucose in ad lib fed B6 mice. C57BL/6J mice were tail-vein injected with adenoviruses expressing GFP, AA-HDAC5-GFP, or HDAC4/5 shRNAs and after 4 days, blood glucose was tested. Data are shown as mean +/- s.e.m.

(C) Glucose tolerance test performed on fasted C57BL/6J mice on normal chow diet tail-vein injected with either scrambled or HDAC4/5/7 shRNA. Data are shown as mean +/- s.e.m. (n= 5), * $p<0.05$, Student's t-test.

Figure S7. Loss of Class IIa HDACs in Ob/Ob Mice Reduces Fasting Blood Glucose, Related to Figure 7

(A) Ten week old ob/ob mice were tail-vein injected with adenoviruses bearing either scramble (scram) shRNA or HDAC4/5/7 (HDAC) shRNAs. 5 days later, mice were fasted for 18h and blood glucose was measured. Average blood glucose value shown in red. Data are shown as mean +/- s.e.m. (n=4). * $p<0.001$ Student's *t*-test.

(B) Ob/ob mice were tail-vein injected with adenoviruses bearing indicated shRNAs. Liver lysates were immunoblotted with indicated antibodies.

EXTENDED EXPERIMENTAL PROCEDURES

Antibodies and Biochemistry

Except where noted, cell and liver extracts were prepared in 20mM Tris pH 7.5, 150mM NaCl, 1mM EDTA, 1 mM EGTA, 1% Triton X-100, 2.5 mM pyrophosphate, 50 mM NaF, 5 mM b-glycero-phosphate, 50 nM calyculin A, 1 mM Na3VO4, 10 mM PMSF, 4 mg/ml leupeptin, 4 mg/ml pepstatin, 4 mg/ml aprotinin) lysis buffer. Total protein was normalized using BCA protein kit (Pierce) and lysates were resolved on SDS-PAGE gel. Cell Signaling Antibodies used: pAMPK Thr172 (#2535), pACC Ser79 (#3661), pRaptor Ser792 (#2083), total Raptor (#2280), total HDAC3 (#3949), total HDAC4 (#2072), total HDAC4 (#5392), total HDAC5, (#2082), pHDAC4 Ser246/HDAC5 Ser259/HDAC7 Ser155 (#3443), phospho-HDAC4 Ser632/HDAC5 Ser498/HDAC7 Ser486 (#3424), total SIRT1 (#2028), LKB1 (#3050), Foxo1 (#2880), Foxo3 (#9467), Phospho-Foxo (#9464), (CREB (#9197), Myc (#2278), Myc (#2276), GST (#2622). Millipore antibodies used: LKB1 (#07-694), Histone3 K9/K14 (#06-599), Acetyl Lysine (#05-515). Santa Cruz antibodies used: Ac Foxo1 (#sc49437), αTubulin (SC53029), HDAC7 H237 (sc-11421). Abcam antibodies used: HDAC3 (ab7030), HDAC3 (ab11967**).** Sigma antibodies used: M2 Flag (#F1804), anti-Flag (#F7425). Anti-CRTC2 and PGC1a was as previously described (Dentin et al., 2009).

Primary Hepatocyte Luciferase Assays

Primary hepatocytes were harvested from wild type C57BL/6J mice and cultured in serum free Medium 199 and infected at 5 PFUs/ cell with scrambled control shRNA, HDACs shRNAs or CRTC2 shRNA (for 72h total). After 24h, cells were co-infected with reporters, CRTC2 WT or HDAC5-AA expressing adenovirus for 40-48h. Cells were treated with either vehicle or 10uM Forskolin for 4 hours and lysed in passive lysis buffer (Promega) and analyzed using Dual-Glo Luciferase Reporter System (Promega) Firefly luciferase signal was normalized to Renilla luciferase or B-galactosidase. All infections and treatments were done in triplicates and readouts were then averaged.

Generated and Purchased Adenoviruses

The following adenoviruses were purchased from Vector Biolabs: Ad-U6-Scramble (scram) RNAi-GFP (#1122), Foxo3A (#1026), Ad-pRenilla-Luc (#1671). pAD GFP was purchased from Eton Bioscience (#0100032001). The following adenoviruses were previously described: pAd RSV-Bgal, pAd G6Pase- luc, pAd CRE-luc, pAd Foxo1 shRNA, pAd CRTC2 shRNA, pAd US scrambled RNAi, pAd wild type CRTC2 (Dentin et al., 2007). pAd CMV CRE was purchased from University of Iowa Gene Transfer Vector Core (Iowa City, IA). GFP Foxo1 WT adenovirus was provided by D. Accili (Columbia Uinversity). GFP HDAC5 WT and GFP HDAC5 S259A/ S498A expressing adenoviruses were generated using the pAd⁄CMV⁄V5-DEST vector of Gateway Cloning Technology (Invitrogen) starting from previously described GFP-HDAC5 constructs. HDAC specific shRNA expressing adenoviruses were generated using pAd BLOCK-iT Adenoviral RNAi Expression System (Invitrogen). Three separate hairpins per gene were generated and tested for knockdown efficiency in preliminary experiments. All Adenoviruses were generated in large scale preps using forty 15cm plates of 293 E4 cells, CsCl purified and functional viral titers were obtained using an Elisa assay for the

detection of hexon, fiber and penton capsid proteins. The following sequences were used to generate mouse specific shRNAs against the Class IIa HDACs:

mHDAC4:
5'-GGTACAATCTCTCTGCCAAATCGAAATTTGGCAGAGAGATTGTACC-3'
3'-CCATGTTAGAGAGACGGTTTAGCTTTAAACCGTCTCTCTAACATGG-5'

mHDAC5:
5'-GGCTCAGACAGGTGAGAAAGACGAATCTTTCTCACCTGTCTGAGCC-3'
3'-CCGAGTCTGTCCACTCTTTCTGCTTAGAAAGAGTGGACAGACTCGG-5'

mHDAC7:
5'-GGGTCGATACTGACACCATCTCGAAAGATGGTGTCAGTATCGACCC-3'
3'-CCCAGCTATGACTGTGGTAGAGCTTTCTACCACAGTCATAGCTGGG-5'

Animal Adenovirus Experiments

shRNA mediated knockdown in mouse livers was done through tail vein injection of mice at 1 x 10^9 PFUs/ mouse for all pAd shRNAs and GFP-HDAC5-AA mutant, 5 x 10^8 PFUs/mouse for G6Pase- luc reporter, and 1 x 10^8 PFUs for RSV-Bgal and Ad-pRenilla-Luc reporters. Livers were harvested or imaged 4-6 days following adenoviral delivery.

qPCR Analysis

<u>qPCR Primers used (5' to 3'):</u>

1. Agxt2l2
Forward Primer: AGAGGGAGGAACATTCATTGACT
Reverse Primer: GGCTCGCATTATTTTGATGGGA

2. PEPCK
Forward Primer: CTGCATAACGGTCTGGACTTC
Reverse Primer: CAGCAACTGCCCGTACTCC

3. Mmd2
Forward Primer: AGTATGAACACGCAGCAAACT
Reverse Primer: TCCCAGTCGTCATCGGACA

4. IGFBP1
Forward Primer: ATCAGCCCATCCTGTGGAAC
Reverse Primer: TGCAGCTAATCTCTCTAGCAC

5. HDAC4
Forward Primer: CAAGGAGAAGGGCAAAGAGA

Reverse Primer: TCCTGCAGCTTCATCTTCAC

6. G6Pase:
Forward Primer ACTGTGGGCATCAATCTCCTC
Reverse Primer CGGGACAGACAGACGTTCAGC

7. SGK1
Forward Primer: CTGCTCGAAGCACCCTTACC
Reverse Primer: TCCTGAGGATGGGACATTTTCA

8. Cyclophilin:
Forward Primer: TGGAGAGCACCAAGACAGACA
Reverse Primer: TGCCGGAGTCGACAATGAT

Microarrays Analysis

Total RNA was extracted using Trizol reagent (Invitrogen) and purity of the RNA was assessed by Agilent 2100 Bioanalyzer. 500 ng of RNA was reverse transcribed into cRNA and biotin-UTP labeled using the Illumina TotalPrep RNA Amplification Kit (Ambion). cRNA was quantified using an Agilent Bioanalyzer 2100 and hybridized to the Illumina mouseRefseq-8v1.1 Expression BeadChip using standard protocols (Illumina). Image data was converted into unnormalized Sample Probe Profiles using the Illumina BeadStudio software and analyzed on the VAMPIRE microarray analysis framework. Stable variance models were constructed for each of the experimental conditions (n=2). Differentially expressed probes were identified using the unpaired VAMPIRE significance test with a 2-sided, Bonferroni-corrected threshold of $\alpha_{Bonf} = 0.05$. The VAMPIRE statistical test is a Bayesian statistical method that computes a model-based estimate of noise at each level of gene expression. This estimate was then used to assess the significance of apparent differences in gene expression between 2 experimental conditions. Lists of altered genes generated by VAMPIRE were mapped to pathways using the VAMPIRE tool GOby to determine whether any KEGG categories were overrepresented using a Bonferroni error threshold of $\alpha_{Bonf} = 0.05$. Heat map was constructed using the CIMminer program at http://discover.nci.nih.gov/, a development of the Genomics and Bioinformatics Group, Laboratory of Molecular Pharmacology (LMP), Center for Cancer Research (CCR) National Cancer Institute (NCI).

Immunoflourescence

Cells were washed three times with PBS and fixed in 4% cold PFA. Anti-Myc (9B11, Cell Signaling Technology #2276) ab was used for detecting Myc-AMPKa2. Secondary antibodies were anti-rabbit Alexa488 and anti-mouse Alexa594 (Molecular Probes, 1:1000). DNA was stained with DAPI. Coverslips were mounted in FluoromountG (SouthernBiothech). Images were acquired on a Zeiss Axioplan2 epifluorescence microscope coupled to the Openlab software. Images were acquired using the 63x objective. Immunoflourescence to detect endogenous Foxo1 and HDAC4 was performed on primary hepatocytes treated either with vehicle (DMSO) or 10uM Forskolin for 1 hr.

Confocal Imaging Analysis Primary hepatocytes were treated either with Vehicle (media) or 100nM Glucagon for indicated times, washed in PBS and fixed with 4% PFA. Confocal microscopy was performed on an LSM 710 spectral confocal microscope mounted on an inverted Axio Observer Z1 frame (Carl Zeiss, Jena, Germany). Excitation for both markers was provided by a 405nm solid-state diode laser (for DAPI) and the 488nm line of an Argon-ion laser (for green) respectively. Laser light was directed to the sample via two separate dichroic beamsplitters (HFT 405 and HFT 488) through a Plan-Apochromat 63X 1.4NA oil immersion objective (Carl Zeiss, Jena Germany). Fluorescence was epi-collected and directed to the detectors via a secondary dichroic mirror. DAPI fluorescence was detected via a photomultiplier tube (PMT) using the spectral window 430-480nm. Green fluorescence was detected on a second photomultipler tube (PMT) with a detection window of 500-570nm. Confocal slice thickness was typically kept at 0.8 microns consistently for both fluorescence channels with 10 slices typically being taken to encompass the three-dimensional entirety of the cells in the field of view. Maximum intensity projections of each region were calculated for subsequent quantification and analysis.

Acetylation Assessment

In vivo: Primary hepatocytes were isolated from wild type C57BL/6J mice and cultured in serum free Medium 199 (Mediatech, 5.5mM glucose) after attachment. Cells were infected with adenoviruses encoding control scrambled shRNA and/or HDAC4/5/7 shRNAs for a total of 72h of knockdown. Cells were transduced with either wild-type Foxo3a or wild-type GFP-Foxo1 expressing adenovirus for 24h prior to cell lysis in scrambled or HDACs shRNAs infected cells. Lysis buffer (20mM Tris pH 7.5, 150mM NaCl, 1mM EDTA, 1 mM EGTA, 1% Triton X-100, 2.5 mM pyrophosphate, 50 mM NaF, 5 mM β-glycero-phosphate, 50 nM calyculin A, 1 mM Na3VO4) contained 5uM TSA and 10mM Nicotinamide. Total protein was normalized by modified BCA protein analysis and resolved on SDS-PAGE gel. Foxo1/3 acetylation and HDAC knockdown was assessed using the above-mentioned antibodies. Endogenous Foxo1 acetylation was assessed in Foxo1 immunoprecipitates from mouse livers expressing scrambled or HDAC4/5/7 shRNAs.

In vitro: The following recombinant proteins were purchased from Enzo Life Sciecnes: recombinant HDAC1 (BML-SE456), HDAC3 (BML-SE507), HDAC3/ NCoR1 (BML-SE515), SIRT1 (BML-SE239). The following recombinant proteins were purchased from Millipore: p300, HAT domain (14-418), HDAC4 (14-828), Foxo1 (14-343). Recombinant HDAC5 (H87-31G) was purchased from SignalChem. Invitro acetylation reactions were performed by incubating 2ug of recombinant GST Foxo1 with recombinant HAT fragment of p300 for 1 hour at 30 degrees. Reactions were carried out in acetylation buffer contatining 50 mM Tris HCl (pH 8.0), 0.1 mM EDTA, 1 mM DTT, 10% glycerol in the in presence of 50uM acetyl Co-A. Acetylated recombinant Foxo1 was bound to GSH beads and beads were washed 2 times in acetylation buffer and 2 times in deacetylation buffer containing 25 mM Tris HCl (pH 8.0), 137 mM NaCl, 2.7 mM KCl, 1mM MgCl2 and incubated with indicated deacetylases for 1 hr at 30 degrees. NAD+ was added to the SIRT1 reaction as previously described (Brunet et al., 2004). Reactions were ran out on SDS - PAGE gel and blotted with indicated antibodies.

Tissue Isolation and Histology
Experimental mice were cervically dislocated and liver was harvested immediately and either processed for histological analysis (10% formalin) or frozen in liquid nitrogen for molecular studies. These samples were then placed frozen into Nunc tubes and homogenized in lysis buffer (20mM Tris pH 7.5, 150mM NaCl, 1mM EDTA, 1 mM EGTA, 1% Triton X-100, 2.5 mM pyrophosphate, 50 mM NaF, 5 mM β-glycero-phosphate, 50 nM calyculin A, 1 mM Na3VO4, Roche complete protease inhibitors) on ice for 30s using a tissue homogenizer. For glycogen assay on mouse liver, 10mg or less of frozen livers of corresponding mice were weighed and homogenized using a 2ml dounce homogenizer and assessed for glycogen content using Glycogen Assay Kit (Biovision). Samples were done in triplicate and read out in triplicates. Data represents the mean +/- SEM. For histology, mouse livers were harvested and fixed in 10% formalin for 24 hrs and then switched to 70% EtOH. Livers were embedded in paraffin and 5 micron liver sections were obtained and stained for hematoxylin and eosin stain or Periodic acid-Schiff (PAS) stain. Slides were viewed on Zeiss microscope and images were taken using CRI Nuance system.

Mouse Luciferase Imaging
Control scrambled shRNA or HDAC shRNAs were co-injected with pAd-G6Pase- luc reporter, pAd-pRenilla-Luc or pAd-RSV-Bgal in 8 week old male C57BL/6J mice. 4 days later, mice were starved for 18h and imaged on IVIS Kinetic 200 from Caliper Life Sciences following 300mg/kg D-luciferin injection and anesthetized using isoflurane. Relative photon counts were normalized comparing control shRNA injected mice to HDAC4/5/7 shRNA injected mice using Living Image 3.2 (as well as to B-gal expression). In vivo imaging experiment was repeated three independent times.

Glucose tolerance tests
Glucose tolerance tests (GTTs) were performed on 10 – 12 week old db/db mice injected with either scrambled or HDAC4/5/7 shRNAs. 7-10 days after adenoviral infection, mice were fasted for 18h overnight, basal fasted blood glucose was measured and mice were injected with 1g glucose per kg (except B6 mice used 2 g glucose per kg) and blood glucose readings were taken at indicated time points. Pyruvate tolerance tests (PTTs): 16 week db/db mice were starved 18h overnight, basal fasting blood glucose was measured and mice were injected with 2 g sodium pyruvate per kg. Blood glucose readings were taken at indicated time points.

SUPPORTING SUPPLEMENTAL TEXT

Supplemental text regarding Class IIa HDACs antisera and their subcellular localization:

To rigorously validate the endogenous proteins detected by immunoblotting, we generated adenoviruses bearing hairpin shRNAs directed against HDAC4, HDAC5, and HDAC7. Similar to Hepa1-6 cells, in cultured primary hepatocytes, as well as in intact livers harvested from mice tail-vein injected with adenoviral shRNAs, endogenous HDAC4 and HDAC5 proteins were readily detected (Figure 1B). Notably, shRNA against HDAC4 or HDAC7 resulted in up-regulation of HDAC5 protein levels, whereas shRNA against HDAC5 or HDAC7 resulted in up-regulation of HDAC4 protein levels, indicating significant compensatory regulatory mechanisms at the protein level. Thus, to study loss of ClassIIa HDAC function in hepatocytes, it is necessary to combine shRNAs to HDAC4, HDAC5, and HDAC7 (Figure 1B). This compensatory upregulation of family members was not observed in the cell lines in Figure S1A.

To examine whether the well-established regulatory phosphorylation sites conserved in Class II HDACs were regulated in these cells, we characterized phospho-specific antibodies against the two best studied sites: Serine259 in HDAC5 (Ser246 in HDAC4/Ser155 HDAC7) and Serine498 in HDAC5 (Ser467 in HDAC4/Ser358 in HDAC7). The importance of these sites in the regulation of 14-3-3 binding and nuclear/ cytoplasmic shuttling of the Class IIa HDACs has been well-established in previous studies (Grozinger and Schreiber, 2000; McKinsey et al., 2000a,b; Wang et al., 2000; Zhao et al., 2001; Vega et al., 2004).

Importantly, the flanking residues recognized by the Phospho-Ser259 antibody are completely conserved between HDAC4 and HDAC5, and differ only by a single subtle residue substitution in HDAC7, allowing these antibodies to detect all three of these Class IIa HDAC family members (Figure 1A,B). Full-length HDAC4 and HDAC5 are similar in molecular weight and migrate at the same position of SDS-PAGE (~140kD), whereas HDAC7 in liver primarily migrates at 105kD (Figure 1B). After verifying the phospho-specificity of the antibodies (Figure S1B), an examination of endogenous HDAC proteins in liver lysates revealed that HDAC4 shRNA resulted in a

loss of ~ 50% of the 140kD band recognized by the Phospho-Ser259 antibody, and similarly HDAC5 shRNA reduced the other 50% of this band. shRNA to both HDAC4 and HDAC5 resulted in a near complete loss of this band, but not of the 105kD band recognized by the antibody which was abolished by HDAC7 shRNA (Figure 1B). These RNAi experiments suggest that endogenous hepatic HDAC4, HDAC5, and HDAC7 are all expressed and recognized by the Ser259 and Ser498 antibodies we are utilizing. It also indicates that the phosphorylation of these three family members is coordinately regulated in murine liver and the cell lines examined.

Importantly, whether AMPK activating compounds alter the subcellular localization of the Class IIa HDACs depends on the basal phosphorylation state of these proteins in the cell line and culture conditions being examined. In growing U2OS osteosarcoma tumor cells, the Class IIa HDACs are not significant basally phosphorylated and are nuclear when overexpressed, hence shuttle in response to AMPK activators (Figure S1C). Importantly, their 14-3-3 association and cytoplasmic shuttling occurs when co-expressed with constitutively active AMPK and is not seen with non-phosphorylatable serine-to-alanine HDAC5 mutants (Figure S1D, S1E). In contrast to U20S cells, in primary hepatocytes and fed murine liver, Class IIa HDACs are fairly highly phosphorylated in the basal state hence the degree of phosphorylation or cytoplasmic shuttling induced by AMPK activation is less than observed in the U2OS cells. Collectively, we expect the localization of Class IIa HDACs and its reliance on AMPK or other LKB1-dependent kinases will rely on the cell line and mostly reflect the expression and activity of the various LKB1-dependent kinases as well as other kinases that can also phosphorylate these sites, including PKD and members of the CAMK family.

Supplemental discussion regarding roles of Class I/II/III HDACs

It remains to be fully elucidated in what contexts the Sirtuins or Class IIa HDAC/HDAC3 complexes modulate FOXO acetylation in liver. As Class IIa HDACs are activated through hormonal increases in cAMP, this may augment or complement the conditions in which the NAD^+-dependent sirtuins may act on FOXO in different tissues (Brunet et al., 2004; Motta et al., 2004; van der Horst et al., 2004). SIRT1 has been

shown to contribute to transcriptional control of glucose and lipid metabolism through the deacetylation of FOXO, PGC1a, HNF4a, SREBP1, STAT3, and LXR amongst other targets (Feige and Auwerx, 2008). Expectantly, hepatic delivery of SIRT1 shRNA has been shown to reduce gluconeogenesis (Rodgers and Puigserver, 2007), though the effect of loss of SIRT1 function in mice on glucose homeostasis varies in different studies (Rodgers and Puigserver, 2007; Chen et al., 2008; Purushotham et al., 2009), which may be due to the strain background of the mice used, the method of SIRT1 depletion, and/or the potential compensation of other sirtuins for loss of SIRT1 function in this process.

Extensive crosstalk is likely to exist between these different metabolic regulatory systems and the interplay between these sensors and hormonal cues is an area of ongoing investigation. For example in muscle, calcium-dependent increases in AMPK activity result in increased SIRT1 activity following exercise (Canto et al., 2009). Notably, the relationship of AMPK and SIRT1 in liver appears more complex, as their control of gluconeogenesis is diametrically opposite here, unlike their function in muscle (Canto and Auwerx, 2010). Critical to understanding how transcriptional control of metabolism changes in response to fasting and refeeding is the realization that individual regulatory modules will be engaged to different extents based on the timing and strength of the signals involved. Thus one might expect one set of responses initially following fasting that involve loss of insulin-dependent post-translational events, as well as initiation of events acutely triggered by fasting hormones such as glucagon, giving rise to events dependent on increased transcriptional output downstream of glucagon. Like shown here for Class IIa HDACs, SIRT1 activity in liver is increased following fasting, though this is occurs at least in part via increased total SIRT1 protein (Rodgers et al., 2005). It is possible that SIRT1 activity may also be controlled post-translationally as well. What will be critical for the field is the development of acetylation site specific antibodies that can recognize the endogenous acetylated versions of these transcriptional regulators so that careful timecourses following fasting and refeeding in liver can be performed. Comparisons of such data to timecourses following glucagon, insulin, and metformin treatment in isolated hepatocytes can be examined to integrate a picture of when different modifications occur temporally during the fasting and feeding

cycle in vivo and ultimately define which HATs and HDACs are functionally under different physiological and pathological conditions. Also critical will be the development of sensitive assays of SIRT1 enzymatic activity and Class IIa/ HDAC3 enzymatic activity immunoprecipitated from tissues at different timepoints or metabolic states. Ultimately, future investigations will better define the relative timing and contributions of Class I, II, and III HDACs in glucose homeostasis and reveal which HDACs and HDAC inhibitors may hold promise as therapeutics for metabolic disease.

SUPPLEMENTAL REFERENCES

Brunet, A., Sweeney, L.B., Sturgill, J.F., Chua, K.F., Greer, P.L., Lin, Y., Tran, H., Ross, S.E., Mostoslavsky, R., Cohen, H.Y.*, et al.* (2004). Stress-dependent regulation of FOXO transcription factors by the SIRT1 deacetylase. Science *303*, 2011-2015.

Canto, C., Gerhart-Hines, Z., Feige, J.N., Lagouge, M., Noriega, L., Milne, J.C., Elliott, P.J., Puigserver, P., and Auwerx, J. (2009). AMPK regulates energy expenditure by modulating NAD+ metabolism and SIRT1 activity. Nature *458*, 1056-1060.

Canto, C., and Auwerx, J. (2010) AMP-activated protein kinase and its downstream transcriptional pathways. Cell Mol Life Sci. PMID: 20640476

Chen, D., Bruno, J., Easlon, E., Lin, S.J., Cheng, H.L., Alt, F.W., and Guarente, L. (2008). Tissue-specific regulation of SIRT1 by calorie restriction. Genes Dev *22*, 1753-1757.

Dentin, R. *et al.* Insulin modulates gluconeogenesis by inhibition of the coactivator TORC2. *Nature* **449**, 366–369 (2007).

Hsiao, A., Ideker, T., Olefsky, J. M., Subramaniam, S. VAMPIRE microarray suite: a web-based platform for the interpretation of gene expression data. *Nucleic Acids Res.* **33**,W627-W632 (2005).

McKinsey, T.A., Zhang, C.L., Lu, J., and Olson, E.N. (2000a). Signal-dependent nuclear export of a histone deacetylase regulates muscle differentiation. Nature *408*, 106-111.

McKinsey, T.A., Zhang, C.L., and Olson, E.N. (2000b). Activation of the myocyte enhancer factor-2 transcription factor by calcium/calmodulin-dependent protein kinase-stimulated binding of 14-3-3 to histone deacetylase 5. Proc Natl Acad Sci U S A *97*, 14400-14405.

Motta, M.C., Divecha, N., Lemieux, M., Kamel, C., Chen, D., Gu, W., Bultsma, Y., McBurney, M., and Guarente, L. (2004). Mammalian SIRT1 represses forkhead transcription factors. Cell

116, 551-563.

Purushotham, A., Schug, T.T., Xu, Q., Surapureddi, S., Guo, X., and Li, X. (2009). Hepatocyte-specific deletion of SIRT1 alters fatty acid metabolism and results in hepatic steatosis and inflammation. Cell Metab *9*, 327-338.

Rodgers, J.T., Lerin, C., Haas, W., Gygi, S.P., Spiegelman, B.M., and Puigserver, P. (2005). Nutrient control of glucose homeostasis through a complex of PGC-1alpha and SIRT1. Nature *434*, 113-118.

Rodgers, J.T., and Puigserver, P. (2007). Fasting-dependent glucose and lipid metabolic response through hepatic sirtuin 1. Proc Natl Acad Sci U S A *104*, 12861-12866.

van der Horst, A., Tertoolen, L.G., de Vries-Smits, L.M., Frye, R.A., Medema, R.H., and Burgering, B.M. (2004). FOXO4 is acetylated upon peroxide stress and deacetylated by the longevity protein hSir2(SIRT1). J Biol Chem *279*, 28873-28879.

Vega, R.B., Harrison, B.C., Meadows, E., Roberts, C.R., Papst, P.J., Olson, E.N., and McKinsey, T.A. (2004). Protein kinases C and D mediate agonist-dependent cardiac hypertrophy through nuclear export of histone deacetylase 5. Mol Cell Biol *24*, 8374-8385.

Zhao, X., Ito, A., Kane, C.D., Liao, T.S., Bolger, T.A., Lemrow, S.M., Means, A.R., and Yao, T.P. (2001). The modular nature of histone deacetylase HDAC4 confers phosphorylation-dependent intracellular trafficking. J Biol Chem *276*, 35042-35048.

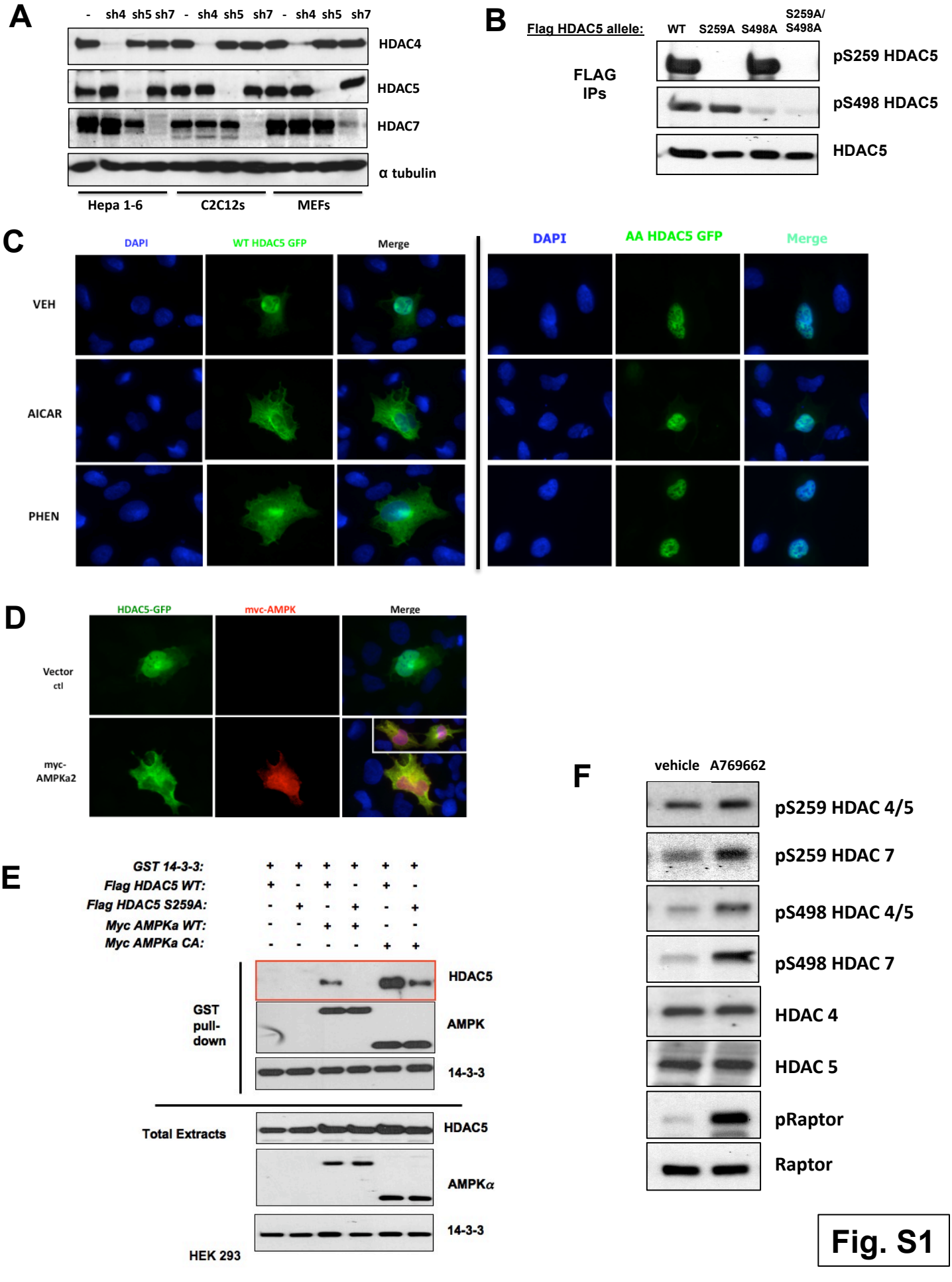
A
- sh4 sh5 sh7 - sh4 sh5 sh7 - sh4 sh5 sh7
HDAC4
HDAC5
HDAC7
α tubulin
Hepa 1-6
C2C12s
MEFs
B
Flag HDAC5 allele:
WT S259A S498A S259A/ S498A
FLAG IPs
pS259 HDAC5
pS498 HDAC5
HDAC5
C
DAPI
WT HDAC5 GFP
Merge
DAPI
AA HDAC5 GFP
Merge
VEH
AICAR
PHEN
D
HDAC5-GFP
myc-AMPK
Merge
Vector ctl
myc-AMPKa2
E
GST 14-3-3:
Flag HDAC5 WT:
Flag HDAC5 S259A:
Myc AMPKa WT:
Myc AMPKa CA:
GST pull-down
HDAC5
AMPK
14-3-3
Total Extracts
HDAC5
AMPKα
14-3-3
HEK 293
F
vehicle A769662
pS259 HDAC 4/5
pS259 HDAC 7
pS498 HDAC 4/5
pS498 HDAC 7
HDAC 4
HDAC 5
pRaptor
Raptor

Fig. S1

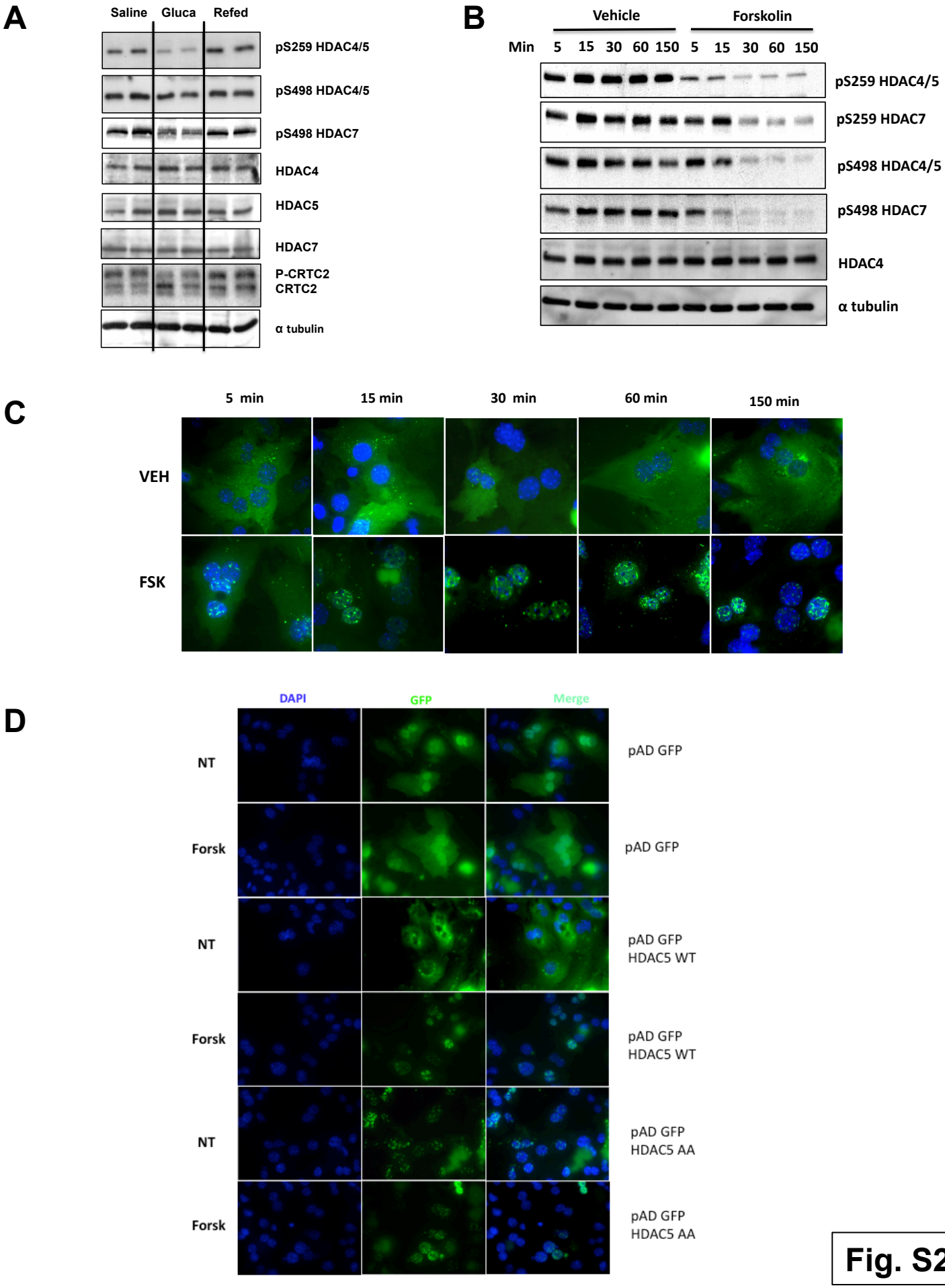
A
Saline
Gluca
Refed
pS259 HDAC4/5
pS498 HDAC4/5
pS498 HDAC7
HDAC4
HDAC5
HDAC7
P-CRTC2
CRTC2
α tubulin
B
Vehicle
Forskolin
Min
5 15 30 60 150 5 15 30 60 150
pS259 HDAC4/5
pS259 HDAC7
pS498 HDAC4/5
pS498 HDAC7
HDAC4
α tubulin
C
5 min
15 min
30 min
60 min
150 min
VEH
FSK
D
DAPI
GFP
Merge
NT
Forsk
NT
Forsk
NT
Forsk
pAD GFP
pAD GFP
pAD GFP
HDAC5 WT
pAD GFP
HDAC5 WT
pAD GFP
HDAC5 AA
pAD GFP
HDAC5 AA

Fig. S2

A

locus	description	ratio of scram/HDAC
G6pc	glucose-6-phosphatase, catalytic	0.032
Sgk1	serum/glucocorticoid regulated kinase 1	0.046
Aldob	aldolase B, fructose-bisphosphate	0.067
Serpina1b	serine (or cysteine) preptidase inhibitor, clade A, member 1B	0.073
Vtn	vitronectin	0.081
Agxt2l1	alanine-glyoxylate aminotransferase 2-like 1	0.1
Cyp1a2	cytochrome P450, family 1, subfamily a, polypeptide 2	0.104
Serpina1b	serine (or cysteine) preptidase inhibitor, clade A, member 1B	0.123
Serpina1a	serine (or cysteine) peptidase inhibitor, clade A, member 1A	0.128
Serpina1a	serine (or cysteine) peptidase inhibitor, clade A, member 1A	0.129
Serpina1d	serine (or cysteine) peptidase inhibitor, clade A, member 1D	0.14
Cyp17a1	cytochrome P450, family 17, subfamily a, polypeptide 1	0.145
Mettl7b	methyltransferase like 7B	0.147
Gstm6	glutathione S-transferase, mu 6	0.149
Sgk1	serum/glucocorticoid regulated kinase 1	0.152
Akr1c19	aldo-keto reductase family 1, member C19	0.153
Serpinf2	serine (or cysteine) peptidase inhibitor, clade F, member 2	0.156
Hdac5	histone deacetylase 5	0.166
Mmd2	monocyte to macrophage differentiation-associated 2	0.17
Bicc1	bicaudal C homolog 1 (Drosophila)	0.172
Sult1a1	sulfotransferase family 1A, phenol-preferring, member 1	0.173
Gpd1	glycerol-3-phosphate dehydrogenase 1 (soluble)	0.185
Gstm1	glutathione S-transferase, mu 1	0.208
Id2	inhibitor of DNA binding 2	0.212
Pah	phenylalanine hydroxylase	0.215

B

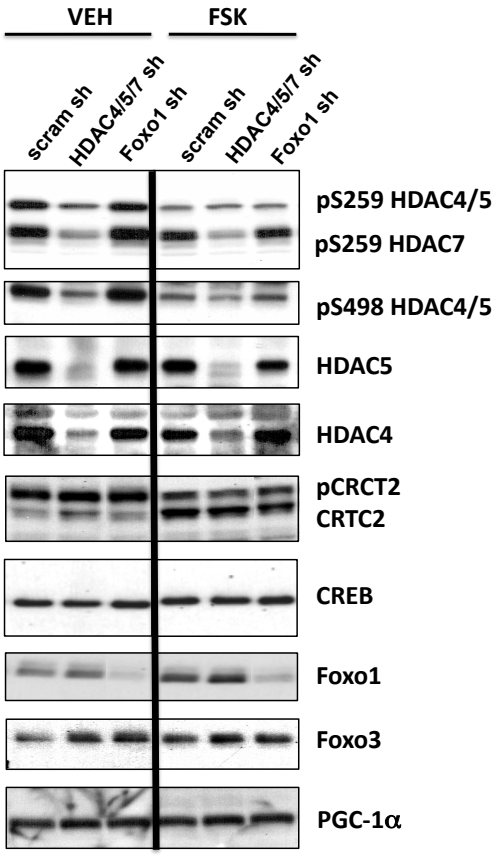

C

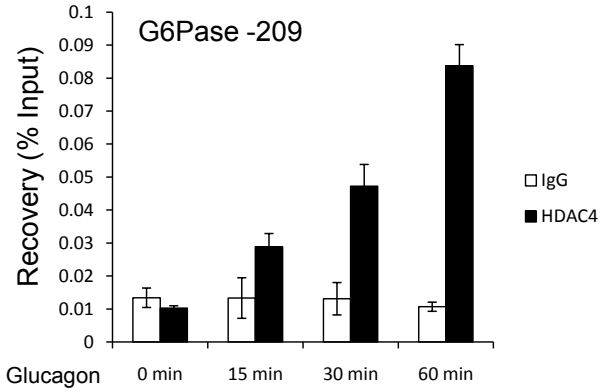

D

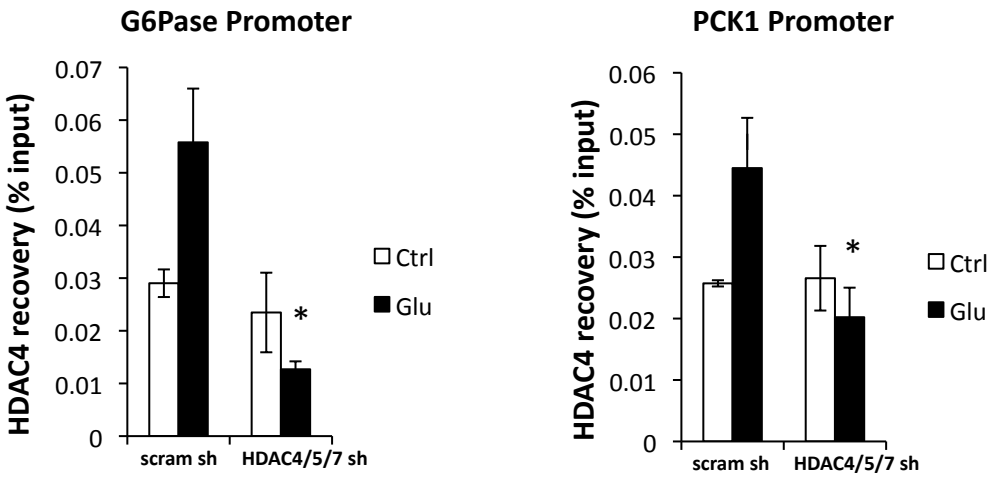

Fig. S3

A

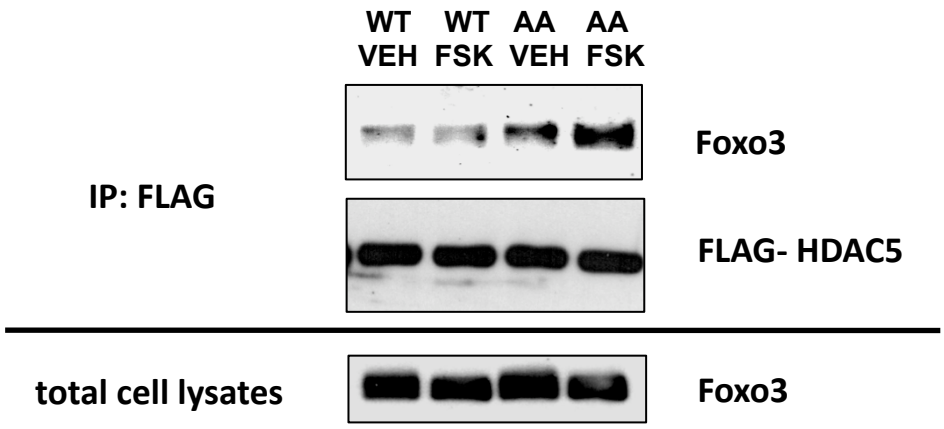
WT VEH
WT FSK
AA VEH
AA FSK
IP: FLAG
Foxo3
FLAG- HDAC5
total cell lysates
Foxo3

B

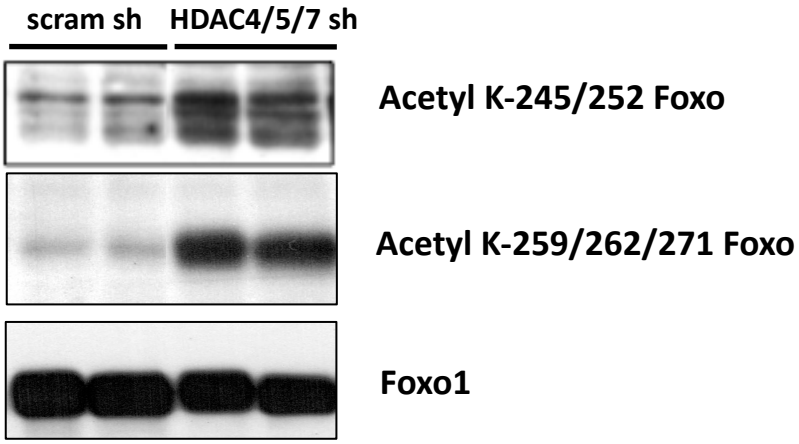
scram sh
HDAC4/5/7 sh
Acetyl K-245/252 Foxo
Acetyl K-259/262/271 Foxo
Foxo1

Fig. S4

A

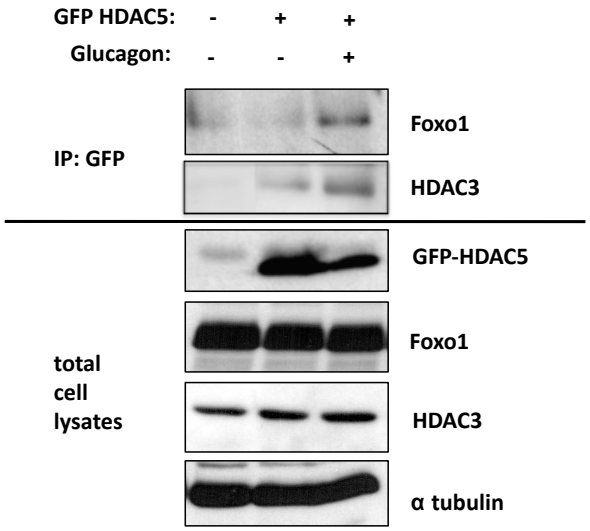
GFP HDAC5: - + +
Glucagon: - - +
IP: GFP
Foxo1
HDAC3
GFP-HDAC5
total cell lysates
Foxo1
HDAC3
α tubulin

B

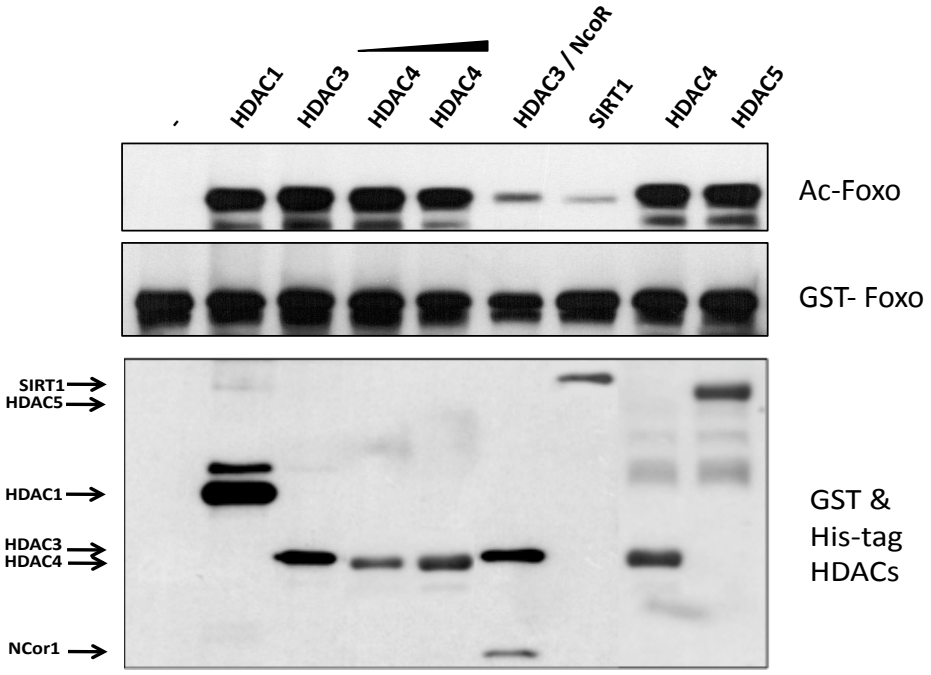
HDAC1
HDAC3
HDAC4
HDAC4
HDAC3 / NcoR
SIRT1
HDAC4
HDAC5
Ac-Foxo
GST- Foxo
SIRT1
HDAC5
HDAC1
HDAC3
HDAC4
NCor1
GST & His-tag HDACs

C

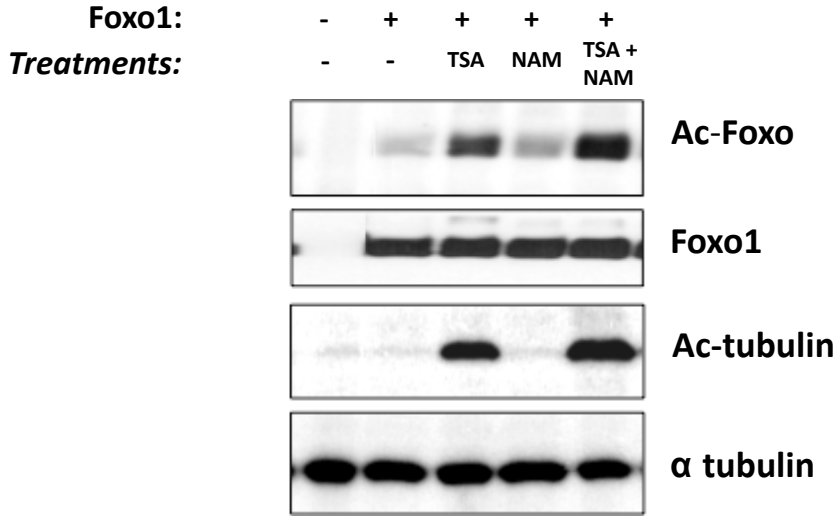
Foxo1: - + + + +
Treatments: - - TSA NAM TSA + NAM
Ac-Foxo
Foxo1
Ac-tubulin
α tubulin

Fig. S5

A

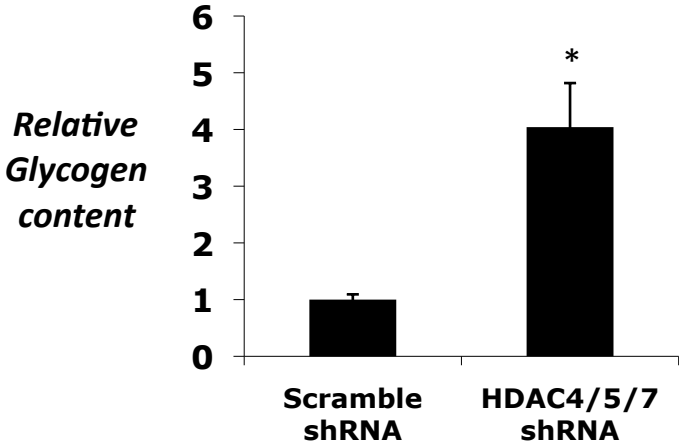
Relative Glycogen content
6
5
4
3
2
1
0
*
Scramble shRNA
HDAC4/5/7 shRNA

B

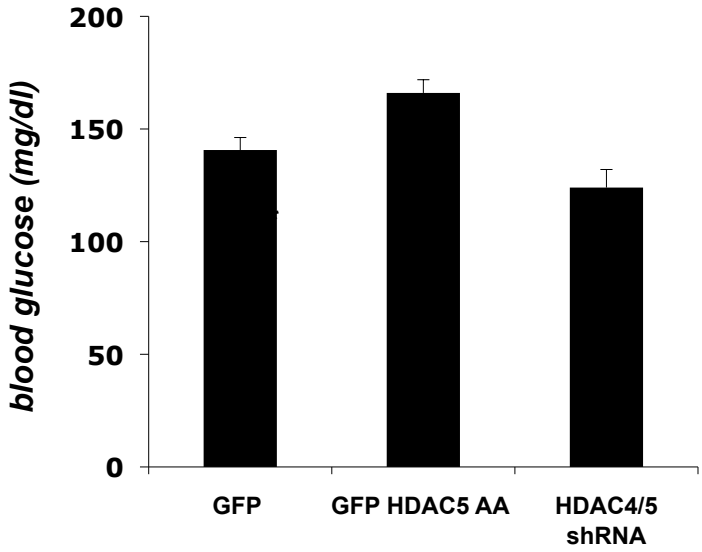
blood glucose (mg/dl)
200
150
100
50
0
GFP
GFP HDAC5 AA
HDAC4/5 shRNA

C

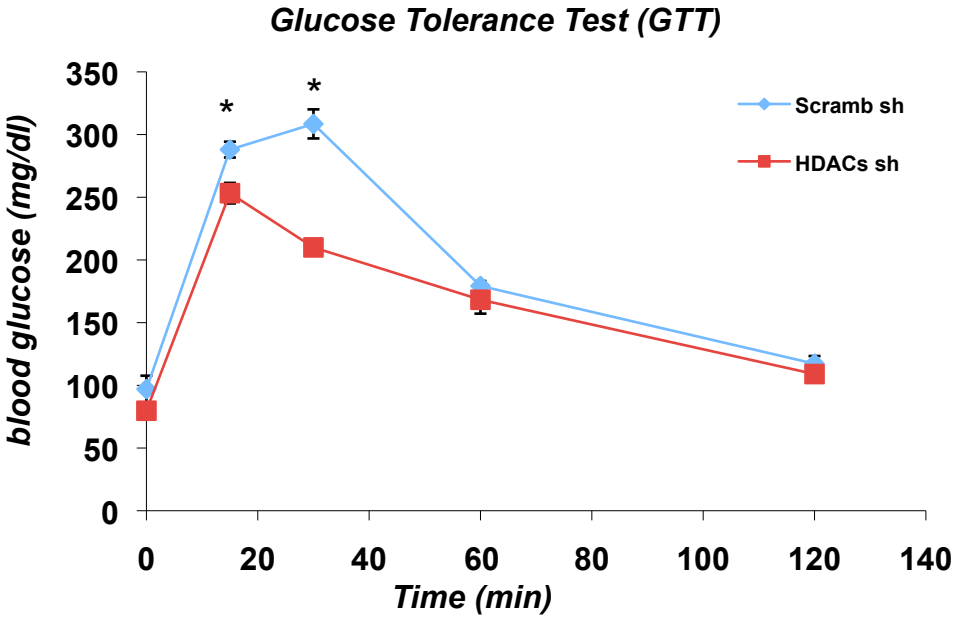
Glucose Tolerance Test (GTT)
blood glucose (mg/dl)
350
300
250
200
150
100
50
0
*
*
Scramb sh
HDACs sh
0
20
40
60
80
100
120
140
Time (min)

Fig. S6

A

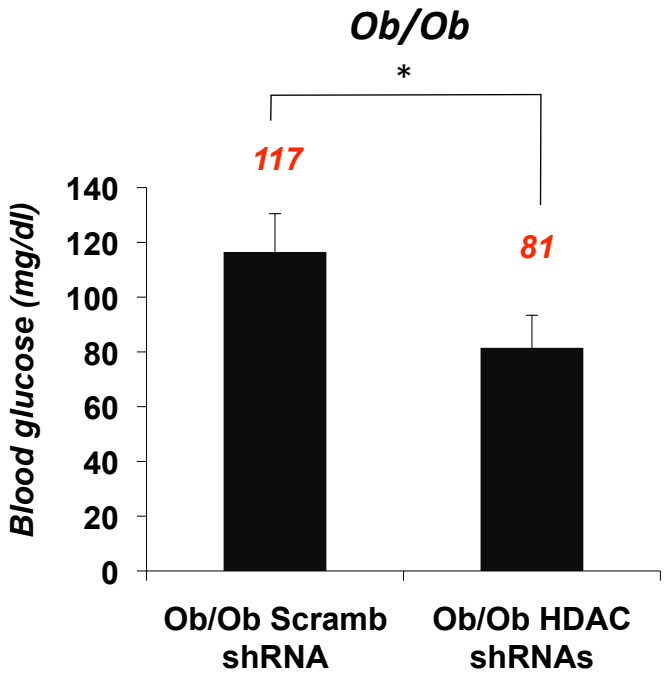
Ob/Ob
*
117
81
Blood glucose (mg/dl)
140
120
100
80
60
40
20
0
Ob/Ob Scramb shRNA
Ob/Ob HDAC shRNAs

B

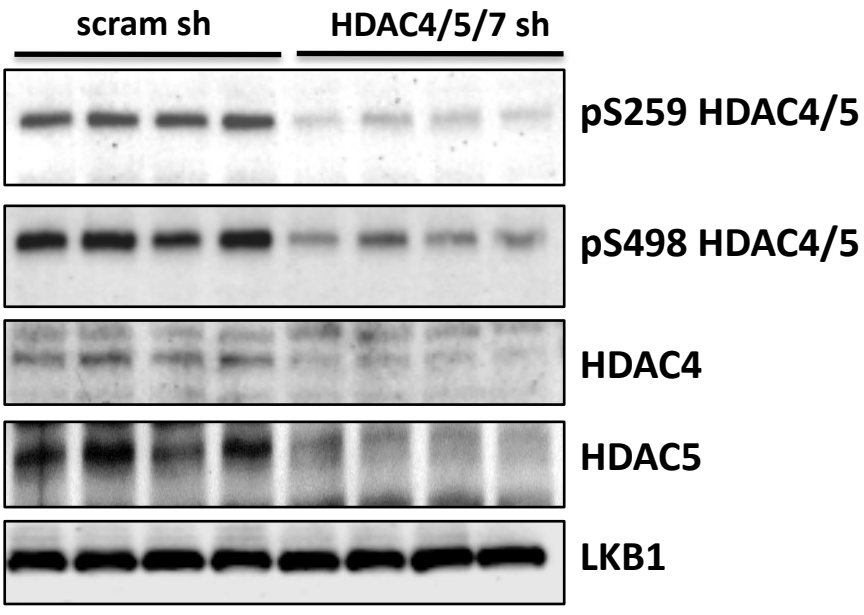
scram sh
HDAC4/5/7 sh
pS259 HDAC4/5
pS498 HDAC4/5
HDAC4
HDAC5
LKB1

Fig. S7